Low-energy electron-impact laser-assisted ionization of atomic hydrogen

A. Makhoute,[1,2] I. Ajana,[1] and D. Khalil[1]
[1]*UFR de Physique du Rayonnement et des Interactions Laser-Matière, Faculté des Sciences, Université Moulay Ismail, B.P. 11201, Zitoune, Meknès, Morocco*
[2]*Abdus Salam International Centre for Theoretical Physics, Strada Costiera II, 34100 Trieste, Italy*
(Received 30 July 2014; published 12 November 2014)

We have studied the influence of a linearly polarized laser field on the dynamics of low (e, $2e$) collisions in atomic hydrogen. The influence of the laser on the target states is treated using a first-order perturbation approach. The continuum states of the scattered and ejected electrons are described respectively by Volkov and Coulomb-Volkov wave functions. The second Born approximation is used to calculate triple differential cross sections for laser-assisted ionization by low-energy electron impact. The required scattering amplitudes are evaluated by using the Sturmian basis expansion. The influence of the laser parameters (photon energy, intensity, and direction of polarization) on the triple differential cross sections is analyzed, and several illustrative examples are discussed. Our second Born approximation results agree very well with those obtained in the first-order Born approximation at larger incident energies. The margins between the second and first Born approximation results are large at low incident energies in the vicinity of the recoil peaks.

DOI: 10.1103/PhysRevA.90.053415 PACS number(s): 34.50.Rk, 34.80.Dp, 34.50.Fa

I. INTRODUCTION

Laser-assisted collision processes find increasing importance from both theoretical and experimental points of view [1–8]. Particularly, the laser-assisted ionization of atoms or ions by charged particles play a very dominant role in many practical fields, such as in the plasma confinement in fusion plasmas, laser heating of plasma [9–11], high-power gas lasers, gas break down, semiconductor physics where the electron-electron collision rate (and hence the transport properties of the system) can be steered by applying an external laser field [12,13], and the development and understanding of ultrafast optoelectronic devices. The rapid development in laser technology combined with the impressive advances in multiparticle detection techniques allowed the realization of the first kinematically complete experiment for the laser-assisted electron-impact ionization [14,15]. The experiment was performed using multiparticle imaging techniques "reaction microscopes" by overlapping a 1-keV pulsed electron beam and a Nd:YAG laser beam at the position of a supersonic helium target beam. The experimental results are compared to the predictions of a first-order Born approximation calculation and clear deviations are observed. The choice of the atomic target is very important to facilitate the comparison between theory and experiment. From the theoretical perspective, atomic hydrogen is ideal due to its analytically known wave functions. Unfortunately, most of the experimental data obtained for the e-H single ionization system are still available only on a relative scale. The difficulty of putting the data on the absolute scale leads to large error bars. On the other side, helium is a much more convenient target for the experimentalists. Consequently, there are a great deal more data available for the e-He single ionization system. These data generally have much smaller statistical error bars and have been mostly put on an absolute scale with considerably less uncertainty than in the case of the atomic hydrogen target. For theorists, on the other hand, helium presents extra difficulties over atomic hydrogen in the treatment of the initial state and spin coupling in the final states. The measurable quantity calculated by theory is the so-called triple differential cross section (TDCS), which depends on the energies and the emission solid angles of the continuum electrons.

At an early stage of this research field, theoretical studies treated this process by neglecting the target dressing effects and described the unbound electrons either as nonrelativistic Volkov or Coulomb-Volkov states [16–22]. Later on, Joachain and coworkers investigated the case of hydrogen [23,24] and helium targets [25,26] while considering the dressing of the atomic states. They found that the dressing of the target by the laser field can significantly affect the TDCSs corresponding to ionizing processes. In these studies, the S-matrix elements were evaluated in the first Born approximation (FBA), which provides a useful tool for capturing the qualitative trends in the measured cross sections. It is usually assumed that the first Born approximation for electron-atom ionization becomes valid at sufficiently high impact energies [27].

Recently, the fully differential cross section for the electron-impact single ionization of atoms (in the absence of laser) at low to intermediate energies has been calculated [28–30]. This motivated us to attempt the present work, which studies the laser-assisted single ionization of hydrogen atom, theoretically the most preferred target, at relatively low impact incident energies, where the energies of the outgoing electrons are more equal. In this domain of incident energy, the first Born approximation is inadequate to treat the projectile-target interaction. In this paper, we present a second Born calculation of the (e, $2e$) triple differential cross section for the laser-assisted ionization of atomic hydrogen by low electrons. The calculation of the required radial amplitudes is performed by expanding the atomic wave functions on to a Sturmian basis, which allows us to exactly take into account the contribution of the continuous spectrum to the dressing of the atomic states. This method of computation constitutes an important advantage over the closure approximation used in the recent study of Zheng *et al.* [31]. We represent the variation of the triple differential cross sections in the coplanar asymmetric geometry. The interaction of the laser field with the unbound electrons is treated in a nonperturbative way using Volkov

wave functions [32], while that of the ejected electron moving in the combined field of the residual ion H^+ and of the laser is obtained by using the ansatz formulated by Joachain *et al.* [23]. We have used the first-order time-dependent perturbation theory to treat the influence of the laser field on the target states.

The present work is structured as follows. In Sec. II, we develop the theory of laser-assisted $(e, 2e)$ reactions of atomic hydrogen in the first and second Born approximations. In Sec. III, we present our numerical results and analysis. Section IV summarizes our conclusions. Unless otherwise stated, atomic units (a.u.) are used throughout.

II. THEORY

We assume the laser field to be classical, monochromatic, linearly polarized, and spatially homogeneous over atomic dimensions. Working in the Coulomb gauge, we have for the electric field $\boldsymbol{\mathcal{E}}(t) = \boldsymbol{\mathcal{E}}_0 \sin(\omega t + \varphi)$ the corresponding vector potential $\boldsymbol{A}(t) = \boldsymbol{A}_0 \cos(\omega t + \varphi)$ with $\mathbf{A}_0 = c\ \boldsymbol{\mathcal{E}}_0/\omega$, where $\boldsymbol{\mathcal{E}}_0$ and ω are the electric field amplitude vector and the laser frequency, respectively. φ denotes the initial phase of the laser field.

The process in the course of which ℓ photons from the laser field are exchanged, while the ionizing electron-atom collision takes place, can be described by the equation

$$e^-(\boldsymbol{k}_i) + \mathrm{H}(1s) + \ell\omega \longrightarrow \mathrm{H}^+ + e^-(\boldsymbol{k}_a) + e^-(\boldsymbol{k}_b), \qquad (1)$$

which presents the collision of an incoming electron of momentum $\boldsymbol{k}_i$, with the hydrogen target (in its ground state) in the presence of an incident laser field.

The energy conservation equation corresponding to the laser-assisted $(e, 2e)$ reaction of Eq. (1) reads

$$E_{k_i} + E_0 + \ell\omega = E_{k_a} + E_{k_b}, \qquad (2)$$

where $E_0 = -0.5$ a.u. is the ground-state energy of atomic hydrogen, while the atomic energy recoil is neglected. $E_{k_i} = k_i^2/2$, $E_{k_a} = k_a^2/2$, and $E_{k_b} = k_b^2/2$ represent, respectively, the kinetic energy of the incident, scattered, and ejected electrons.

The time-dependant Schrödinger equation for the nonrelativistic incident and scattered electrons embedded in a laser field can be exactly solved, giving the well-known Volkov wave function [32]

$$\chi_k(\boldsymbol{r}_0,t) = (2\pi)^{-\frac{3}{2}} \exp\{i[\boldsymbol{k}\cdot\boldsymbol{r}_0 - \boldsymbol{k}\cdot\boldsymbol{\alpha}_0 \sin(\omega t) - E_k t]\}, \qquad (3)$$

where $\boldsymbol{k}$ denotes the electron wave vector, $E_k = k^2/2$ is its kinetic energy, and $\boldsymbol{\alpha}_0 = \frac{\boldsymbol{\mathcal{E}}_0}{\omega^2}$ is the amplitude of oscillation of a classical electron in the laser field.

On the other hand, the dressed wave function of the atomic target in the laser field corresponding to the initial bound state is obtained in the first-order time-dependant perturbation theory [4]

$$\phi_n(\boldsymbol{r}_1,t) = e^{-iE_n t} e^{-i\mathbf{a}\cdot\mathbf{r}_1} \left[\psi_n(\boldsymbol{r}_1) + \frac{i}{2} \sum_{n'} \left(\frac{e^{i\omega t}}{\omega_{n'n} + \omega} - \frac{e^{-i\omega t}}{\omega_{n'n} - \omega} \right) M_{n'n}\ \psi_{n'}(\boldsymbol{r}_1) \right], \qquad (4)$$

where $\boldsymbol{r}_1$ is the target coordinate, ψ_n is a target state of energy E_n in the absence of the external field, $\omega_{n'n} = E_{n'} - E_n$ is the Bohr frequency, and $\mathbf{a} = \boldsymbol{A}/c$ where $e^{-i\mathbf{a}\cdot\mathbf{r}_1}$ is a gauge factor. Furthermore, we have defined

$$M_{n'n} = M^*_{nn'} = \boldsymbol{\mathcal{E}}_0 \cdot \langle \psi_{n'} | \boldsymbol{r} | \psi_n \rangle \qquad (5)$$

as the dipole-coupling matrix element. We note that if one specializes Eq. (4) to the ground state ϕ_0 and if the ground state is spherically symmetric, then the sum in Eq. (4) runs only over the discrete and continuum hydrogen atom p states ψ_{np}.

For the dressed continuum wave function representing the state of the ejected electron moving in the field of residual ion and in the presence of the laser field, we have used the wave function proposed by Joachain *et al.* [23,24]

$$\phi_{k_b}(\boldsymbol{r}_1,t) = e^{-iE_{k_b}t} e^{-i\boldsymbol{a}\cdot\boldsymbol{r}_1} e^{-i\boldsymbol{k}_b\cdot\boldsymbol{\alpha}_0 \sin(\omega t)} \times \left[\psi^{(-)}_{c,k_b}(\boldsymbol{r}_1)[1 + i\boldsymbol{k}_b\cdot\boldsymbol{\alpha}_0 \sin(\omega t)] + \frac{i}{2} \sum_n \left(\frac{e^{i\omega t}}{E_n - E_{k_b} + \omega} - \frac{e^{-i\omega t}}{E_n - E_{k_b} - \omega} \right) \times M_{nk_b} \psi_n(\boldsymbol{r}_1) \right], \qquad (6)$$

where $\psi^{(-)}_{c,k_b}(\boldsymbol{r}_1)$ is a modified continuum Coulomb wave function with incoming spherical wave behavior, corresponding to momentum $\boldsymbol{k}_b$ and normalized to a δ function in momentum space.

In the case of high laboratory intensities (which still $\mathcal{E}_0 \ll \frac{e}{a_0^2}$) and low laser frequencies, the perturbative results given by Eq. (6) should be modified in order to account for strong coupling which is characteristic of the interaction between an unbound particle and an intense external field in infrared limit. For this purpose and for more details see [18] and references therein.

The central quantity to be evaluated is therefore the direct FBA S-matrix element

$$\mathbf{S}^{B_1}_{\mathrm{ion}} = -i \int_{-\infty}^{+\infty} dt \big\langle \chi_{k_a}(\boldsymbol{r}_0,t)\Phi_{k_b}(\boldsymbol{r}_1,t) \big| V_d(\boldsymbol{r}_0,\boldsymbol{r}_1) \times |\chi_{k_i}(\boldsymbol{r}_0,t)\Phi_0(\boldsymbol{r}_1,t)\rangle, \qquad (7)$$

In this equation $V_d(\boldsymbol{r}_0,\boldsymbol{r}_1) = \frac{1}{|\boldsymbol{r}_0 - \boldsymbol{r}_1|} - \frac{1}{r_0}$, r_0 and r_1 are, respectively, the projectile and target electron coordinates. Using Eqs. (3), (4), and (6) one finds that the FBA S-matrix element can be recast in the form

$$S^{B_1}_{\mathrm{ion}} = (2\pi)^{-1} i \sum_{\ell=-\infty}^{\ell=+\infty} \delta\big(E_{k_a} + E_{k_b} - E_{k_i} - E_0 - \ell\omega\big)\ f^{B_1,\ell}_{\mathrm{ion}}, \qquad (8)$$

where $f^{B_1,\ell}_{\mathrm{ion}}$ is the first Born approximation to the $(e, 2e)$ scattering amplitude with the transfer of ℓ photons. This quantity is given by

$$f^{B_1,\ell}_{\mathrm{ion}} = f_1 + f_2 + f_3, \qquad (9)$$

with

$$f_1 = -2\Delta^{-2} J_l(\lambda)\langle\psi^{(-)}_{c,k_b}|\exp(i\,\boldsymbol{\Delta}\cdot\mathbf{r})|\psi_0\rangle, \tag{10a}$$

$$f_2 = i\,\Delta^{-2}\sum_n \langle\psi^{(-)}_{c,k_b}|\exp(i\,\boldsymbol{\Delta}\cdot\mathbf{r})|\psi_n\rangle \times M_{n0}\left(\frac{J_{\ell-l}(\lambda)}{E_n - E_0 - \omega} - \frac{J_{\ell+l}(\lambda)}{E_n - E_0 + \omega}\right), \tag{10b}$$

and

$$f_3 = i\,\Delta^{-2}\sum_n \langle\psi_n|\exp(i\,\boldsymbol{\Delta}\cdot\mathbf{r})|\psi_0\rangle \times M^*_{nk_b}\left(\frac{J_{\ell-l}(\lambda)}{E_n - E_{k_b} + \omega} - \frac{J_{\ell+l}(\lambda)}{E_n - E_{k_b} - \omega}\right) - 2\Delta^{-2}\boldsymbol{k}_b\cdot\boldsymbol{\alpha}_0 J'_\ell(\lambda)\langle\psi^{(-)}_{c,k_b}|\exp(i\,\boldsymbol{\Delta}\cdot\mathbf{r})|\psi_0\rangle. \tag{10c}$$

In these equations, J_ℓ is an ordinary Bessel function of order ℓ, $\boldsymbol{\Delta} = \boldsymbol{k}_i - \boldsymbol{k}_a$ is the momentum transfer, and we have introduced the quantity $\lambda = (\boldsymbol{\Delta} - \boldsymbol{k}_b)\cdot\boldsymbol{\alpha}_0$.

The first Born triple differential cross section corresponding to the $(e, 2e)$ reaction (1) accompanied by the transfer of ℓ photons is given by

$$\frac{d^3\sigma^{B_1,\ell}_{\rm ion}}{d\Omega_a\, d\Omega_b\, dE} = \frac{k_a k_b}{k_i}\left|f^{B_1,\ell}_{\rm ion}\right|^2, \tag{11}$$

and we remark that the results obtained by Cavaliere *et al.* [17] can be recovered from the present treatment by keeping only the first term f_1 of Eq. (9).

Similarly, the second-order term in the direct interaction potential reads

$$S^{B_2}_{\rm ion} = -i\int_{-\infty}^{+\infty} dt\int_{-\infty}^{+\infty} dt'\langle\chi_{k_a}(\boldsymbol{r}_0,t)\phi_{k_b}(\boldsymbol{r},t)|V_d(\boldsymbol{r}_0,\boldsymbol{r}) \times G^{(+)}_0(\boldsymbol{r}_0,\boldsymbol{r},t,\boldsymbol{r}'_0,\boldsymbol{r}',t') \times V_d(\boldsymbol{r}'_0,\boldsymbol{r}')|\chi_{k_i}(\boldsymbol{r}'_0,t')\phi_0(\boldsymbol{r}',t')\rangle, \tag{12}$$

where $G^{(+)}_0$ is the causal propagator defined by

$$G^{(+)}_0(\boldsymbol{r}_0,\boldsymbol{r},t,\boldsymbol{r}'_0,\boldsymbol{r}',t') = -i\Theta(t-t')\sum_n\int d\boldsymbol{q}\,\chi_q(\boldsymbol{r}_0,t) \times \chi_q(\boldsymbol{r}'_0,t')\phi_n(\boldsymbol{r},t)\phi_n(\boldsymbol{r}',t'), \tag{13}$$

It should be noted that this term is second order in the electron-atom interaction potential V_d, and contains atomic wave functions corrected to first-order correction in $\mathcal{E}_0$ for the target dressed states. If one retains a global first-order correction in $\mathcal{E}_0$ for the target states, one finds that $S^{B_2}_{\rm ion}$ is the sum of two terms which are respectively of zeroth and first order in $\mathcal{E}_0$. We shall neglect the second-order contribution to the S-matrix element for laser-assisted collisions calculated in first order in $\mathcal{E}_0$, and concentrate our discussion on the computation of the dominant term $S^{B_2,0}_{\rm ion}$, which describes the collision of a Volkov electron with the undressed atom.

Thus, it turns out that the lowest-order component $S^{B_2,0}_{\rm ion}$ evaluated at the shifted momenta $\boldsymbol{\Delta}_i = \boldsymbol{k}_i - \boldsymbol{q}$ and $\boldsymbol{\Delta}_f = \boldsymbol{q} - \boldsymbol{k}_a$ can be expressed in terms of the simpler second Born amplitude (SBA) as

$$S^{B_2,0}_{\rm ion} = -(2\pi)^{-1} i\sum_{\ell=-\infty}^{\ell=+\infty}\delta\big(E_{k_a} - E_{k_b} - E_{k_i} - E_0 - \ell\omega\big) f^{B_2,\ell,0}_{\rm ion}(\boldsymbol{\Delta}), \tag{14}$$

with

$$f^{B_2,\ell,0}_{\rm ion}(\boldsymbol{\Delta}) = -\frac{J_\ell(\lambda)}{\pi^2}\int_0^{+\infty} q^2 dq\, d\xi_q \times \frac{\langle\psi^{(-)}_{c,k_b}|\widetilde{V}_d(\boldsymbol{\Delta}_f,\boldsymbol{r})G_c(\xi)\widetilde{V}_d(\boldsymbol{\Delta}_i,\boldsymbol{r})|\psi_0\rangle}{\Delta_i^2\Delta_f^2}. \tag{15}$$

The electron-atom amplitude with the transfer of ℓ photons may be written in the second Born approximation as

$$f^{\ell}_{\rm ion}(\boldsymbol{\Delta}) = f^{B_1,\ell}_{\rm ion}(\boldsymbol{\Delta}) + f^{B_2,\ell,0}_{\rm ion}(\boldsymbol{\Delta}), \tag{16}$$

where the first-order term $f^{B_1,\ell}_{\rm ion}(\boldsymbol{\Delta})$ is given by Eq. (9),

$$G_c(\xi) = \sum_n \frac{|\psi_n\rangle\langle\psi_n|}{\xi - E_n} \tag{17}$$

is the Coulomb Green's function with argument $\xi = E_{k_i} + E_0 - E_q - E_{k_b} + \ell\omega$, and we have used the definition $\lambda = \boldsymbol{\alpha}_0.(\boldsymbol{\Delta} - \boldsymbol{k}_b)$ with $\boldsymbol{\Delta} = \boldsymbol{\Delta}_i + \boldsymbol{\Delta}_f$.

In Eq. (16) and according to the expansion (15), we may write the second-order amplitude $f^{B_2,\ell,0}_{\rm ion}(\boldsymbol{\Delta})$ in the form

$$f^{B_2,\ell,0}_{\rm ion}(\boldsymbol{\Delta}) = J_\ell(\lambda) f^{B_2}_{\rm ion}(\boldsymbol{\Delta}), \tag{18}$$

where

$$f^{B_2}_{\rm ion}(\boldsymbol{\Delta}) = -\frac{1}{\pi^2}\int_0^{+\infty} q^2\, dq\, d\xi_q \times \frac{\langle\psi^{(-)}_{c,k_b}|\widetilde{V}_d(\boldsymbol{\Delta}_f,\boldsymbol{r})G_c(\xi)\widetilde{V}_d(\boldsymbol{\Delta}_i,\boldsymbol{r})|\psi_0\rangle}{\Delta_i^2\Delta_f^2}. \tag{19}$$

is the field-free second Born ionization amplitude evaluated at the shifted momenta $\boldsymbol{\Delta}_i$ and $\boldsymbol{\Delta}_f$.

We note that the integral in Eq. (19) over the virtual projectile states $\chi_q(\mathbf{r}_0,t)$, with wave vector $\boldsymbol{q}$, is prohibitively difficult, which is actually zero at some values of incident electron energies. We shall overcome this difficulty by using the exact upper boundary of the integral (19) over the virtual projectile energies, which is obtained by the requirement [33]

$$E_q \leqslant \inf\big(E_{k_i}, E_{k_a}\big). \tag{20}$$

The first and second Born amplitudes corresponding to the first- and second-order contributions to the S-matrix element, for the laser-assisted electron-impact ionization, have been computed exactly without further approximation with the help of a Sturmian approach, similar to that described in [25,34]. This method of computation constitutes an important advantage in the present context with earlier computations relying on the closure approximation [4,5,35,36].

Finally, the second Born triple differential cross section corresponding to the ionization process, with the transfer of ℓ

photons, is given by

$$\frac{d^3\sigma_{\rm ion}^{B_2,\ell}}{d\Omega_a\, d\Omega_b\, dE} = \frac{k_a k_b}{k_i}\left(\frac{1}{4}\left|f_{\rm ion}^{\ell} + g_{\rm ion}^{\ell}\right|^2 + \frac{3}{4}\left|f_{\rm ion}^{\ell} - g_{\rm ion}^{\ell}\right|^2\right). \tag{21}$$

$g_{\rm ion}^{\ell}$ is the first Born exchange amplitude with the transfer of ℓ photons,

$$g_{\rm ion}^{\ell}(\mathbf{\Delta}) \simeq J_{\ell}(\lambda) g_{\rm ion}^{\rm Och}, \tag{22}$$

where $g_{\rm ion}^{\rm Och}$ is the Ochkur amplitude calculated in the absence of the field [37].

III. RESULTS AND DISCUSSION

Let us turn to a discussion of the new results obtained in the case of $(e, 2e)$ collisions in several geometrical configurations. Our calculations focus on the case of atomic hydrogen, for which difficulties arising from the choice of the target wave function and the motion of the ejected electron in the field of the ion are not present. Note, however, that though simplified, the model contains all the ingredients needed for the discussion of the physics of such processes. In the present investigation, our results are interpreted by estimating the first and second Born triple differential cross sections, where the scattering angle is kept fixed at 5°.

In this section, we present and analyze our findings for the TDCS of the laser-assisted $(e, 2e)$ reaction in the coplanar asymmetric geometry. Without loss of generality, we assume the origin of the coordinate system to be the target nucleus and the z axis to be along the incident momentum. The x axis is in the plane defined by the incident momentum and the polarization vector of the external field. The scattering angle of the scattered electron and the emission angle of the ejected electron are denoted, respectively, by θ_a and θ_b. The former is measured in anticlockwise direction, and the latter clockwise.

In Fig. 1, we give the triple differential cross sections corresponding to the laser-assisted electron-impact ionization of a hydrogen target as a function of the incident electron energies, where the angle of the ejected electron is kept fixed. The polarization vector of the field $\hat{\varepsilon}$ (which is along $\boldsymbol{\mathcal{E}}_0$ for the case of linear polarization considered here) is set parallel to the impact momentum $\boldsymbol{k}_i$. The complete results obtained by using the ionization amplitude equations (9) and (16) for the first and second Born approximations are compared with those obtained from the simplified nonperturbative analysis of Cavaliere *et al.* [17] (results obtained by neglecting the dressing of the target which coincide with the electronic amplitude f_1) and with field-free results. It is interesting to note that the results are notably sensitive to the second Born approximation at low incident electron energies. As the incident energy increases, the ratio of the second Born triple differential cross section to the first one becomes smaller, and at high incoming energies such proportionality factor is completely absent, where the second Born approximation does not offer a significant improvement over the first Born treatment.

According to the domain of validity of the treatment used for taking into account the laser-atom interaction, the Nd-YAG

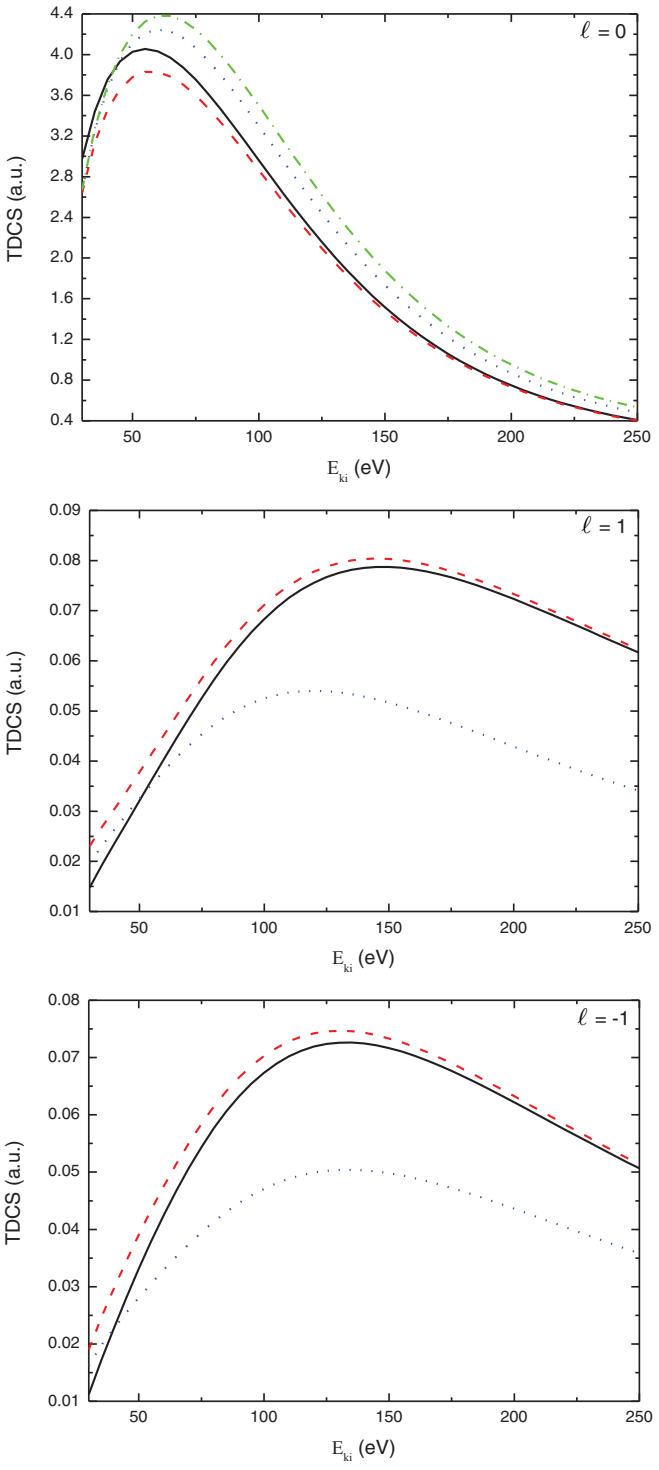

FIG. 1. (Color online) Triple differential cross sections corresponding to the laser-assisted electron-impact ionization process of atomic hydrogen as a function of the incident electron energy. The laser frequency is 1.17 eV, the electric field strength is 10^7 V/cm. The ejected electron energy is $E_{k_b} = 5$ eV, and the scattering angle is $\theta_a = 5°$. The laser polarization of the field is set parallel to the incident momentum $\boldsymbol{k}_i$. Solid lines: second Born approximation results. Dashed lines: first Born approximation results. Dotted lines: results obtained by neglecting the dressing of the target. Dashed dotted lines: field-free results.

laser frequency is taken to be $\hbar\omega = 0.043$ a.u. For no net transfer of photons ($\ell = 0$), our results of TDCS are nearly of the same order of magnitude as field-free TDCS, while for $|\ell| = 1$ the field-free results are much larger (not presented here in our figures). This results from the fact that the laser itself does not contribute to the ionizing process. In fact, the laser redistributes the ejected electrons in new channels associated with indices $\ell \neq 0$ in the energy conservation relation, Eq. (2), which are accessible in the dressed continuum of the atomic target. One observes significant departures of the results obtained by the simplified treatment of Cavaliere with respect to those obtained by the first and second born approximations. This difference in magnitude is traced to the role played by the explicit introduction of the atomic-state dressing of which the contribution was neglected by Cavaliere *et al.* This directly reflects the role of the dressing of the projectile target system by the external laser field. This is one of the interesting typical signatures of the dressing of the electron-target system in the TDCS which clearly shows the effects of the internal structure of the atomic target. Such a distorted atom also acts on the projectile by a long-range dipole potential ($\sim 1/r^2$), which requires a nonperturbative treatment of laser-atom interactions. The long-range dipole potential affects mainly the distant collisions, which contribute when the energies of the primary electron are weak. Another interesting point is the fact that the overall magnitude of the cross sections corresponding to the difference between SBA and FBA decreases with the increase of the incident electron energies. Moreover, our second and first Born TDCSs present an absolute maximum corresponding to the zero of the momentum transfer (i.e., $1/\Delta^2$) contained in various TDCS expressions. The same remark appears in the results obtained by using the simplified approach of Cavaliere and laser-off.

Figures 2 and 3 shows triple differential cross sections versus the field amplitude. Apparently, the $(e, 2e)$ reaction process can be controlled by the field strength. Two special geometries of laser polarization are considered: $\hat{\varepsilon}_0 || \boldsymbol{k}_i$ (the laser polarization vector parallel to the incident momentum) and $\hat{\varepsilon}_0 \perp \boldsymbol{k}_i$ (the laser polarization vector perpendicular to the incident momentum). For no net exchange of photons, the margins between the results of the first and second Born approximations reaches maxima at several values of field strengths in the case of $\hat{\varepsilon}_0 || \boldsymbol{k}_i$, while for $\hat{\varepsilon}_0 \perp \boldsymbol{k}_i$ the margin occurs at weak field strength and at $\mathcal{E}_0 = 7 \times 10^7$ V/cm. Note that for both geometries, dressing effects become very important with the increase of the field strength, this is because the stronger the laser is, the more the atomic states are distorted. The second-order correction is seen to be significant in the vicinity of the maxima of the peaks and decreases with the increase of the laser field amplitude. We also observe a small influence of the laser field at low field strength with the net exchange of photons. This is due to the chosen geometry that coincides approximatively with the region of the binary peak. This situation changes in the recoil peak region, with even a weak field strength, leads to sizable changes in the cross section.

In Figs. 2 and 3, the corresponding dispersion curves in terms of $\mathcal{E}_0$ are characterized by the occurrence of sharp maxima separated by deep minima. The number of lobes increases with the laser intensity. This behavior can be traced back to the

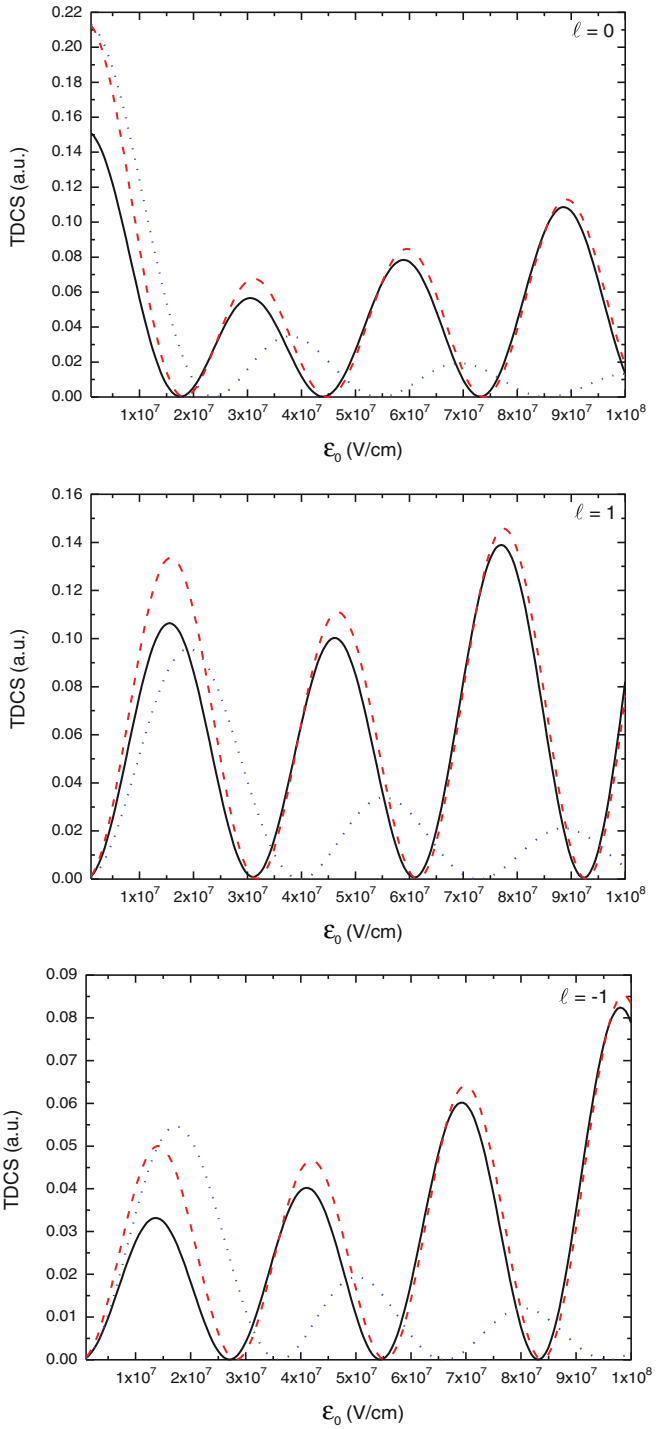

FIG. 2. (Color online) Triple differential cross sections corresponding to the laser-assisted electron-impact ionization process of atomic hydrogen as a function of the amplitude vector. The laser frequency is 1.17 eV, the incident electron energy is $E_{k_i} = 30$ eV, and the ejected electron energy is $E_{k_b} = 5$ eV. The scattering angle is $\theta_a = 5^\circ$, and the emission angle of the ejected electron is $\theta_b = 130^\circ$. The laser polarization of the field is set parallel to the incident momentum $\boldsymbol{k}_i$. Solid lines: second Born approximation results. Dashed lines: first Born approximation results. Dotted lines: results obtained by neglecting the dressing of the target.

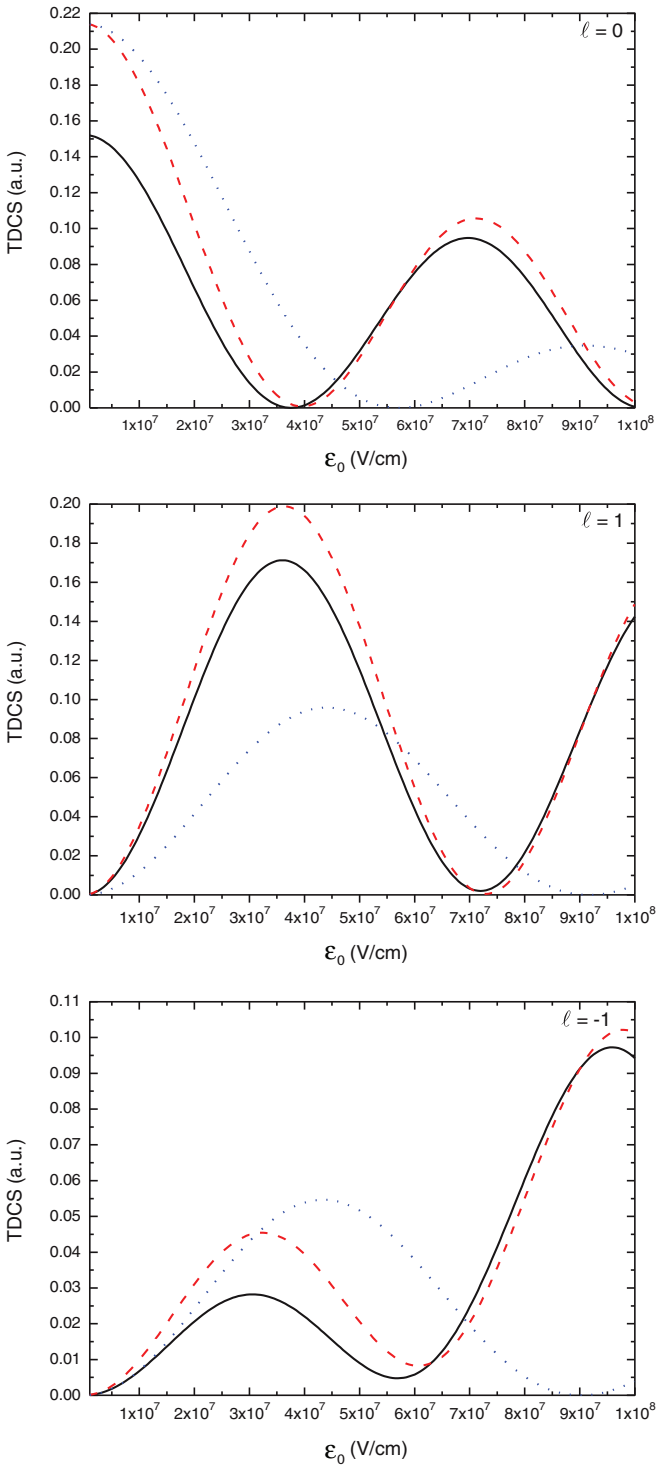

FIG. 3. (Color online) All the parameters are the same as Fig. 2, while the laser polarization is perpendicular to the incident momentum $\boldsymbol{k}_i$.

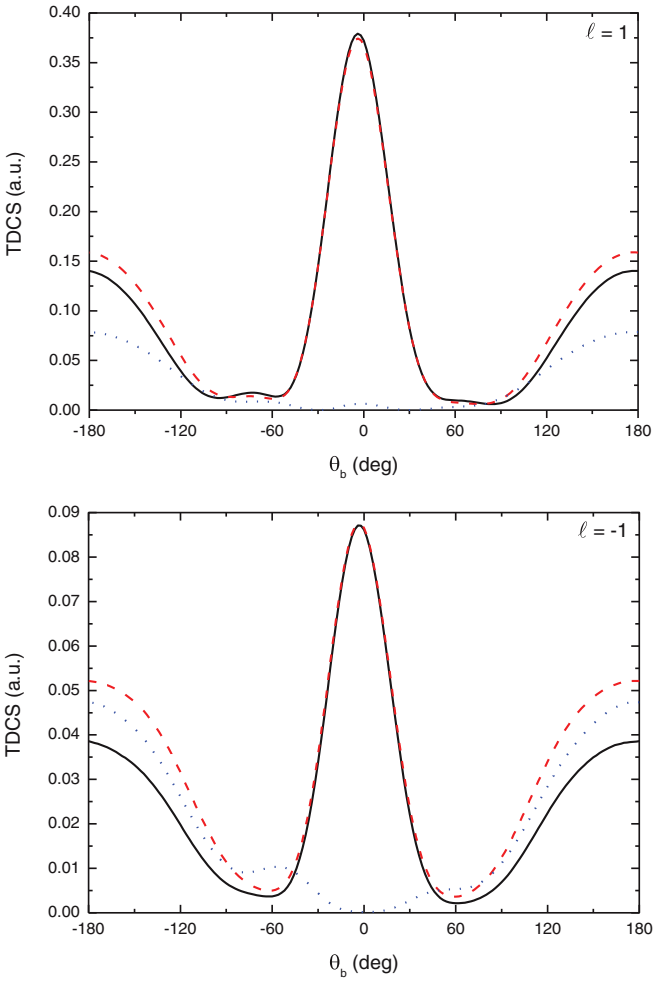

FIG. 4. (Color online) Triple differential cross sections corresponding to the laser-assisted electron-impact ionization process of atomic hydrogen as a function of the ejected angle θ_b. The laser frequency $\omega = 1.17$ eV and the electric field strength is 10^7 V/cm. The incident electron energy is $E_{k_i} = 30$ eV, the ejected electron energy is $E_{k_b} = 5$ eV, and the scattering angle is $\theta_a = 5^\circ$. The laser polarization of the field is set parallel to the incident momentum $\boldsymbol{k}_i$. Solid lines: second Born approximation results. Dashed lines: first Born approximation results. Dotted lines: results obtained by neglecting the dressing of the target.

fact that the argument of the Bessel functions $J_\ell(\lambda)$, entering the expressions of the amplitudes in Eqs. (10) and (15), grows with $\mathcal{E}_0$. By comparing Figs. 2 and 3, one observes that changing the polarization orientation significantly affects the triple differential cross sections. Indeed, the amplitudes $f_{\rm ion}^{B_2,\ell,0}$ and $f_{\rm ion}^{B_1,\ell}$ depend on the laser polarization direction in a quite intricate way since $\hat{\varepsilon}_0$ enters their expressions though the second-order matrix elements and also via the scalar products $\boldsymbol{\alpha}_0 \cdot \boldsymbol{\Delta}$ and $\boldsymbol{\alpha}_0 \cdot \boldsymbol{k}_b$. Dressing effects, i.e., the contributions of the amplitudes f_2 and f_3 in Eqs. (10b) and (10c) significantly affect the TDCS corresponding to the ionizing process. This observation is applied well to the SBA where the contribution of the correction term is seen to be important and improves TDCS calculations.

In Figs. 4–6, we give the triple differential cross sections corresponding to the ionization of atomic hydrogen from the ground state by electron impact, in the presence of a laser field, as a function of the ejected electron angle θ_b. The incident electron energy is $E_{k_i} = 30$ eV, the ejected electron energy is $E_{k_b} = 5$ eV, and the scattering angle is $\theta_a = 5^\circ$. We are working in a geometry in which the polarization vector $\hat{\varepsilon}_0$ of the field is parallel to the incident momentum $\boldsymbol{k}_i$. We present the results of our complete computation of the TDCS in the second Born

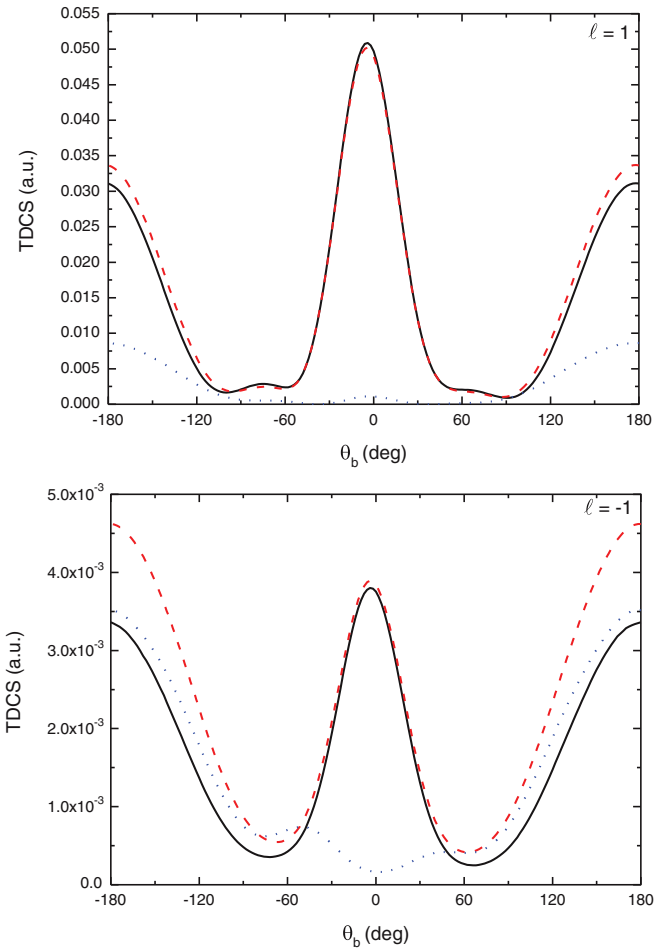

FIG. 5. (Color online) Same as Fig. 4, but with the laser frequency $\omega = 2.34$ eV.

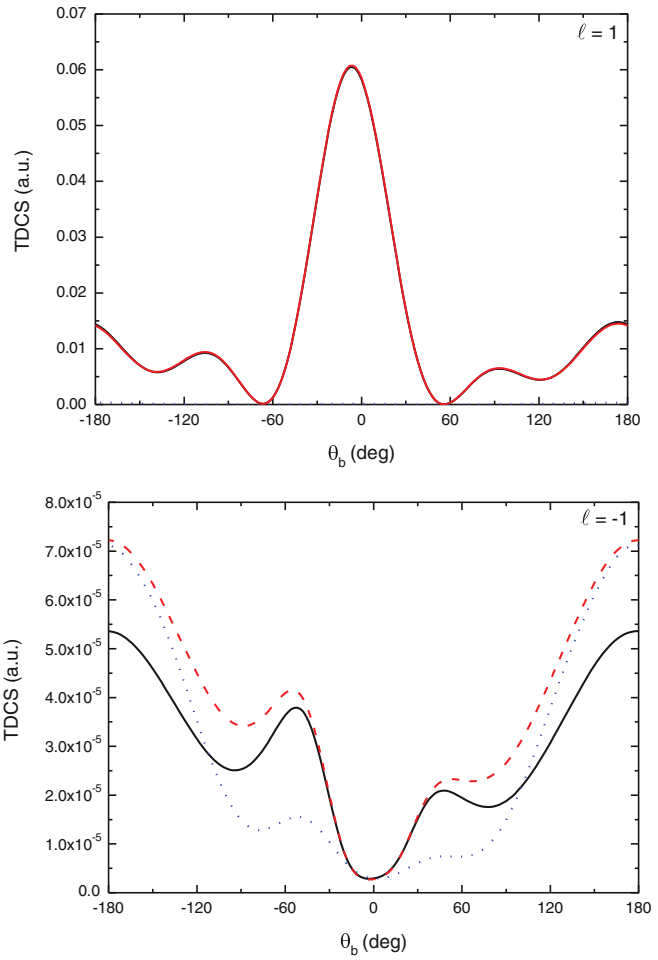

FIG. 6. (Color online) Same as Fig. 4, but with the laser frequency $\omega = 6.42$ eV.

approximation, and compare them with the FBA ones, and with those obtained by neglecting the dressing effects by the laser field. One notices that dressing effects have a relatively large effect on the cross sections with the exchange of one photon ($\ell = \pm 1$). The frequency regimes also have controlling effects on the collision process. In Fig. 4, we observe that the binary peak remains unchanged for the first and second term of the Born series, while the recoil peak is suppressed. Furthermore, the binary peak is dominant and the magnitude of the cross sections is considerably smaller when ($\ell = -1$) compared to the case of the absorption of a photon ($\ell = 1$).

Let us now consider the case of higher frequency lasers. The preceding discussion remains qualitatively valid as long as the condition $\omega < E_{k_b}$ is satisfied. This is well illustrated by our results presented in Figs. 4 and 5 which display the angular distribution for the frequencies $\omega = 1.17$ eV and $\omega = 2.34$ eV. By comparing these results, one observes that the shapes of the angular distributions are mostly the same, the main difference lying in the overall magnitude of the TDCS. Indeed, if everything else is kept fixed, the frequency is increased by a factor of 2, and the electric field coupling parameter α_0 is four times smaller, which correspondingly affects the magnitude of the cross sections. The high-frequency regime where $\omega > E_{k_b}$ is satisfied leads to strong modifications of the angular distribution of the ejected electron. This is confirmed by the results given in Fig. 6 for $\omega = 6.42$ eV and $E_{k_b} = 5$ eV. One observes a typical splitting of the binary and recoil peaks. For the absorption of one photon $\ell = 1$, the margins between SBA and FBA results are negligible, but for the case of emission $\ell = -1$, the modification is large. In fact, the margins between the SBA and FBA results are large except in the vicinity of the binary peak where the two curves coincide. As seen in Fig. 6, at a given field strength, the overall magnitude of the TDCS for $\ell = -1$ is smaller by three orders of magnitude than in the case of $\ell = 1$.

The results displayed in this paper show that the photon absorption processes dominate the photon emission ones, meaning that the system absorbs net energy from the laser field background. The curves for ℓ and $-\ell$ present similar features since $J_{-\ell}(\lambda) = (-1)^{\ell} J_{\ell}(\lambda)$. Nevertheless, the magnitudes of the cross sections for ℓ and $-\ell$ are different. The origin of this difference lies in terms of different expressions of (e, $2e$) scattering amplitudes other than $J_{\ell}(\lambda)$. The cross sections in Figs. 2 and 3 for both geometries are different. In both cases, the oscillation structure in the results is determined by the Bessel function entering the expressions of the ionization amplitudes. When the argument λ and the order ℓ are approximately equal, the value of the function $J_{\ell}(\lambda)$ diminishes

rapidly. Physically, in the extreme case where $\boldsymbol{\Delta} - \boldsymbol{k}_b$ is very small, e.g., when the nucleus is a spectator during the collision, λ is as well very small and the laser field plays a minor role. This is because the energy absorbed by the electrons from the radiation field needs to be converted into a linear momentum via a rescattering from the massive residual ion. Small $|\Delta - k_b|$ means that the rescattering did not take place and hence the weak influence of the laser field on the outcome of the collision process. For large $|\Delta - k_b|$, the scattering processes take place near the nucleus and hence the probability for the electrons to experience a violative transition is generally much higher, except for $\lambda = 0$ (the electric field is $\perp$ to $\boldsymbol{\Delta} - \boldsymbol{k}_b$).

IV. CONCLUSION

The laser-assisted electron-impact ionization $(e, 2e)$ collisions in atomic hydrogen were studied in the second Born approximation. This work is an attempt to study the laser-assisted ionization process in the case of low incident energy. Our treatment consistently includes the dressing of the atomic target by the laser field. We have clearly demonstrated the inadequacy of simplified treatments in which the dressing effects are not included. We have investigated the role of the laser parameters: field strength, frequency, and polarization orientation. It has been shown that dramatic changes in the triply differential cross sections can occur when varying these parameters. At low incident electron energies, the second-order correction is seen to be important and significant at the recoil peak, while it is negligible in the vicinity of the binary peak. Up to now, no laser-assisted $(e, 2e)$ experiment on atomic hydrogen is yet available in the literature. The absence of any experimental data adds further importance to the theoretical study of such a process. We believe that our results should serve as an incentive to perform such laser-assisted collision experiments.

[1] B. Wallbank and J. K. Holmes, J. Phys. B **27**, 1221 (1994).
[2] S. Luan, R. Hippler, and H. O. Lutz, J. Phys. B **24**, 3241 (1991).
[3] B. Wallbank and J. K. Holmes, Can. J. Phys. **79**, 1237 (2001).
[4] F. W. Byron, Jr., P. Francken, and C. J. Joachain, J. Phys. B **20**, 5487 (1987).
[5] P. Francken, Y. Attaourti, and C. J. Joachain, Phys. Rev. A **38**, 1785 (1988).
[6] M. H. Mittleman, *Introduction to the Theory of Laser—Atom Interactions* (Plenum, New York, 1993).
[7] P. Francken and C. J. Joachain, J. Opt. Soc. Am. B **7**, 554 (1990).
[8] F. Ehlotzky, A. Jaroń, and J. Z. Kamiński, Phys. Rep. **297**, 63 (1998).
[9] A. V. Brantov and V. Yu. Bychenkov, Plasma. Phys. Rep. **39**, 698 (2013).
[10] F. Wang, E. Weckert, and B. Ziaja, J. Plasma. Phys. **75**, 289 (2009).
[11] A. Brantov, W. Rozmus, R. Sydora, C. E. Capjack, V. Yu. Bychenkov, and V. T. Tikhonchuk, Phys. Plasmas. **10**, 3385 (2003).
[12] H. Haug and A. P. Jauho, *Quantum Kinetics in Transport and Optics of Semiconductors* (Springer, Berlin, 1996).
[13] R. Dörner, Th. Weber, M. Weckenbrock, A. Staudte, M. Hattass, H. Schmidt-Böcking, R. Moshammer, and J. Ullrich, Adv. At. Mol. Opt. Phys. **48**, 1 (2002).
[14] C. Höhr, A. Dorn, B. Najjari, D. Fischer, C. D. Schröter, and J. Ullrich, Phys. Rev. Lett. **94**, 153201 (2005).
[15] C. Höhr, A. Dorn, B. Najjari, D. Fischer, C. D. Schröter, and J. Ullrich, J. Electron Spectrosc. Relat. Phenom. **161**, 172 (2007).
[16] M. Mohan and P. Chand, Phys. Lett. A **65**, 399 (1978).
[17] P. Cavaliere, G. Ferrante, and C. Leone, J. Phys. B **13**, 4495 (1980).
[18] J. Banerji and M. H. Mittleman, J. Phys. B **14**, 3717 (1981).
[19] P. Cavaliere, C. Leone, R. Zangara, and G. Ferrante, Phys. Rev. A **24**, 910 (1981).
[20] R. Zangara, P. Cavaliere, C. Leone, and G. Ferrante, J. Phys. B **15**, 3881 (1982).
[21] M. Zarcone, D. L. Moores, and M. R. C. McDowell, J. Phys. B **16**, L11 (1983).
[22] S. K. Mandal and A. S. Ghosh, Phys. Rev. A **30**, 2759 (1984).
[23] C. J. Joachain, P. Francken, A. Maquet, P. Martin, and V. Véniard, Phys. Rev. Lett. **61**, 165 (1988).
[24] P. Martin, V. Véniard, A. Maquet, P. Francken, and C. J. Joachain, Phys. Rev. A **39**, 6178 (1989).
[25] D. Khalil, A. Maquet, R. Taïeb, C. J. Joachain, and A. Makhoute, Phys. Rev. A **56**, 4918 (1997).
[26] A. Makhoute, D. Khalil, A. Maquet, and R. Taïeb, J. Phys. B **32**, 3255 (1999).
[27] S. Jones and D. H. Madison, Phys. Rev. A **66**, 062711 (2002).
[28] J. Colgan, M. S. Pindzola, G. Childers, and M. A. Khakoo, Phys. Rev. A **73**, 042710 (2006).
[29] A. T. Stelbovics, I. Bray, D. V. Fursa, and K. Bartschat, Phys. Rev. A **71**, 052716 (2005).
[30] Y. Wang, L. Jiao, and Y. Zhou, Phys. Lett. A **376**, 2122 (2012).
[31] M-Y. Zheng and S-M. Li, Phys. Rev. A **82**, 023414 (2010).
[32] D. M. Volkov, Z. Phys. **94**, 250 (1935).
[33] M. Bouzidi, A. Makhoute, D. Khalil, A. Maquet, and C. J. Joachain, J. Phys. B **34**, 737 (2001).
[34] R. Taïeb, V. Véniardt, A. Maquet, S. Vucic, and R. M. Potvliege, J. Phys. B **24**, 3229 (1991).
[35] F. W. Byron, Jr. and C. J. Joachain, J. Phys. B **17**, L295 (1984).
[36] P. Francken and C. J. Joachain, Phys. Rev. A **35**, 1590 (1987).
[37] F. W. Byron, Jr. and C. J. Joachain, Phys. Rep. **179**, 211 (1989).